

# MicroRNA-494 Is a Master Epigenetic Regulator of Multiple Invasion-Suppressor MicroRNAs by Targeting Ten Eleven Translocation 1 in Invasive Human Hepatocellular Carcinoma Tumors

Kuang-Hsiang Chuang,<sup>1,2,3</sup> Christa L. Whitney-Miller,<sup>4</sup> Chin-Yi Chu,<sup>5,6</sup> Zhongren Zhou,<sup>4</sup> M. Katherine Dokus,<sup>2</sup> Shannon Schmit,<sup>2</sup> and Christopher T. Barry<sup>1,2</sup>

Vascular invasion provides a direct route for tumor metastasis. The degree to which microRNA (miRNA) expression plays a role in tumor vascular invasion is unclear. Here, we report that miR-494 is up-regulated in human hepatocellular carcinoma (HCC) tumors with vascular invasion and can promote HCC cell invasiveness by gene inactivation of multiple invasion-suppressor miRNAs. Our results show that ten eleven translocation (TET) methylcytosine dioxygenase, predominantly TET1 in HCC cells, is a direct target of miR-494. The reduced 5'-hydroxymethylcytosine levels observed in the proximal cytosine-phosphate-guanine (CpG) regions of multiple invasion-suppressor miRNA genes are strongly associated with their transcriptional repression upon miR-494 overexpression, whereas enforced DNA demethylation can abolish the repression. Furthermore, TET1 knockdown shows a similar effect as miR-494 overexpression. Conversely, miR-494 inhibition or enforced TET1 expression is able to restore invasion-suppressor miRNAs and inhibit miR-494-mediated HCC cell invasion. **Conclusions:** miR-494 can trigger gene silencing of multiple invasion-suppressor miRNAs by inhibiting genomic DNA demethylation by direct targeting of TET1, thereby leading to tumor vascular invasion. (HEPATOLOGY 2015;62:466-480)

Hepatocellular carcinoma (HCC) is one of the most common cancers and the third-most common cause of cancer-related death worldwide.<sup>1</sup> Curative therapy through liver transplantation (LT) or hepatic resection is possible only in a minority of patients, namely, those with small tumor burdens and well-compensated underlying liver disease.<sup>2</sup> However, 5-year recurrence rates stand at 70% after tumor resection and 15%-30% post-LT, often leading to mortality.<sup>3</sup>

Vascular invasion is an immediately premetastatic phase during malignant tumor progression. As a tumor

progresses, it may acquire the ability to invade vessel walls, leading to vascular invasion of portal or hepatic veins, resulting in intrahepatic recurrence and/or systemic metastases. It is one of the most critical predictors of HCC recurrence.

MicroRNAs (miRNAs) are endogenous small non-coding RNAs that control target gene expression by messenger RNA (mRNA) degradation or translation inhibition.<sup>4</sup> Aberrant expression of certain miRNAs has been found to be closely correlated with tumor phenotype, suggesting that certain miRNAs might

*Abbreviations:* 5'-Aza, 5'-aza-2'-deoxycytidine; 5hmC, 5'-hydroxymethylcytosine; 5mC, 5-methylcytosine; CpG, cytosine-phosphate-guanine; DNMTs, DNA methyltransferases; EMT, epithelial-mesenchymal transition; FBS, fetal bovine serum; FFPE, formalin-fixed, paraffin embedded; gDNA, genomic DNA; HCC, hepatocellular carcinoma; IDH, isocitrate dehydrogenase; LT, liver transplantation; MCC, mutated in colorectal cancer; miRNA, microRNA; mRNA, messenger RNA; PTEN, phosphatase and tensin homolog; qRT-PCR, quantitative real-time quantitative polymerase chain reaction; RNAi, RNA interference; snoRNA, small nucleolar RNA; TET, ten eleven translocation; UTR, untranslated region; ZEB, zinc-finger E-box binding homeobox.

From the <sup>1</sup>The Wilmot Cancer Institute, University of Rochester Medical Center, Rochester, NY; <sup>2</sup>Department of Surgery Research, University of Rochester Medical Center, Rochester, NY; <sup>3</sup>Department of Radiation Oncology, University of Rochester Medical Center, Rochester, NY; <sup>4</sup>Department of Pathology and Laboratory Medicine, University of Rochester Medical Center, Rochester, NY; <sup>5</sup>Division of Neonatology and Center for Pediatric Biomedical Research, University of Rochester Medical Center, Rochester, NY; <sup>6</sup>Pediatric Molecular and Personalized Medicine Program, University of Rochester Medical Center, Rochester, NY

Received September 30, 2014; accepted March 27, 2015.

Additional Supporting Information may be found at <http://onlinelibrary.wiley.com/doi/10.1002/hep.27816/supinfo>

This work was supported by the Roche Organ Transplant Research Fund (# 871634732) and the Wilmot Cancer Institute.

function as oncogenes or tumor suppressors.<sup>5-7</sup> The pleiotropic nature of miRNAs suggests that multiple signaling and metabolic pathways can be affected by aberrant miRNA expression, thereby significantly directing cancer cell biological behavior.

Aberrant miRNA expression could, in part, be caused by deregulation of upstream transcription factors and epigenetic regulators that control their expression.<sup>5,8</sup> Particularly, gene inactivation of miRNAs by DNA hypermethylation or histone modification has been observed.<sup>9-11</sup> A common epigenetic aberration in cancer involves deregulated DNA methylation such as cytosine-phosphate-guanine (CpG) island hypermethylation that leads to gene silencing of specific tumor-suppressor genes.<sup>12,13</sup>

The ten eleven translocation (TET) family of methylcytosine dioxygenases, including TET1, TET2, and TET3, can convert 5-methylcytosine (5mC) to 5'-hydroxymethylcytosine (5hmC), and remove existing methylation tags in cells.<sup>14-16</sup> In particular, the 5hmC level, closely correlated with the gene expression of the TET family of methylcytosine dioxygenases, is increased in differentiated cells and drastically reduced in many cancer types, indicating that 5hmC level is inversely associated with tumor progression.<sup>17,18</sup> Recently, it has been observed that a gradual decrease of 5hmC and TET1 is associated with progression of HCC tumors and increase of 5mC level positively correlates with HCC tumor invasion and recurrence,<sup>19</sup> suggesting that the DNA methylation/demethylation status, controlled by the TET family of methylcytosine dioxygenases, may impact HCC tumor invasion and recurrence. In this study, we show that miR-494 is up-regulated in human invasive HCC tumors and cell lines, leading to repression of TET gene expression and subsequent transcriptional silencing through CpG hypermethylation of multiple invasion-suppressor miRNA genes.

## Materials and Methods

**Clinical Sample Collection and Histological Confirmation.** Our study was performed with approval of the University of Rochester Research Subjects

Review Board (RSRB00029467). A total of 172 tumor nodules were studied from a cohort of 86 HCC patients who underwent LT at the University of Rochester Medical Center (Rochester, NY) between 1996 and 2008. Patients were well matched with regard to etiology, gender, and age. Patients in the nonrecurrent group tended to have less vascular invasion, lower-grade tumors, and earlier tumor stage, compared to the recurrent group. Representative hematoxylin and eosin sections of the formalin-fixed, paraffin embedded (FFPE) blocks from explanted tumors were reviewed by our pathologist (C.W.-M.) to determine grade and assess for presence or absence of vascular invasion in each tumor nodule. Tissue cores (7-mm diameter) or curls were then obtained from the corresponding blocks and re-embedded for miRNA purification.

**MiRNA Isolation and Microarray Analysis.** MiRNA was isolated from FFPE HCC tumors using the Roche High Pure miRNA isolation kit (Roche Diagnostics, Mannheim, Germany). miRNA extraction was carried out from individual tissue blocks using seven sections of 10 microns each. One to four extractions were carried out for each tumor to generate sufficient miRNA for microarray analysis. All samples were assessed for enriched miRNA using an Experion Bioanalyzer (Bio-Rad, Hercules, CA). MiRNAs were then labeled using the FlashTag Biotin RNA labeling kit (Affymetrix, Santa Clara, CA, USA) by following the manufacturer's protocol and then hybridized to Affymetrix GeneChip miRNA 1.0 microarrays (Affymetrix). These arrays are comprised of 46,228 probe sets representing over 6,703 miRNA sequences (71 organisms) from the Sanger miRNA database (V.11) and an additional 922 sequences of human small nucleolar RNA (snoRNA) and small Cajal body-specific RNA from the Ensemble database and snoRNABase. Array hybridization, washing, and staining was carried out at the Upstate Medical University (Syracuse, NY) microarray core facility, per the manufacturer's instructions, and arrays were scanned with a GeneChip Scanner 7G Plus. Data files (.cel files) were generated using the miRNA-1\_0\_2X gain library file. Array signal

Address reprint requests to: Kuang-Hsiang Chuang, Ph.D., Department of Radiation Oncology, University of Rochester Medical Center, 601 Elmwood Avenue, Rochester, NY 14642. E-mail: KuangHsiang\_Chuang@urmc.rochester.edu; fax: +1-585-276-1201 or Christopher T. Barry, M.D., MOHAN Foundation, 267 Kipauk Garden Road, Chennai 600010, India. E-mail: cbarrymdphd@gmail.com; fax: +91-044-26263477.

Copyright © 2015 The Authors. HEPATOLOGY published by Wiley Periodicals, Inc., on behalf of American Association for the Study of Liver Diseases. This is an open access article under the terms of the Creative Commons Attribution-NonCommercial License, which permits use, distribution, and reproduction in any medium, provided the original work is properly cited and is not used for commercial purposes.

View this article online at [wileyonlinelibrary.com](http://wileyonlinelibrary.com).

DOI 10.1002/hep.27816

Potential conflict of interest: Nothing to report.

intensities and present calls were produced by using the AffyMetrix miRNA QCTool program (version 1.0.33.0; Affymetrix). The normalization algorithm used was the default setting in the AffyMetrix miRNA QCTool program, which is background adjustment, BC-CG Adjust; normalization, Quantile; summarization, median polish. Data processing was carried out on all 46,228 probe sets, after which nonhuman probe sets were removed, leaving 847 human miRNA probe sets. All data have been deposited onto the Gene Expression Omnibus (GEO accession no.: GSE67140; <http://www.ncbi.nlm.nih.gov/geo/>). Differentially expressed miRNAs were selected according to the following criteria: The fold change was no less than 1.5 and *P* value was less than 0.05 by Student *t* test. We also only keep analysis transcripts with a coefficient of variability between 0 and 1 in each group. Hierarchical clustering of variance-normalized expression values was carried out with MeV (v4.9) software (<http://www.tm4.org/mev.html>) using the metric of Pearson's distance and average linkage.

**Cell Migration and Invasion Assays.** Cells ( $5 \times 10^4$  cells) were suspended in 100  $\mu$ L of growth medium containing 1% fetal bovine serum (FBS). For migration assay, cells were loaded in the upper well of the transwell chamber (8-mm pore size; Corning, Corning, NY), with the lower well filled with 600  $\mu$ L of medium containing 10% FBS. For invasion assay, the upper well of the transwell chamber was precoated with 10  $\mu$ g/mL of growth-factor-reduced BD Matrigel matrix (BD Biosciences, San Diego, CA). After incubation for 24 hours at 37°C, noninvaded cells on the upper surface of the filter were removed with a cotton swab, and migrated cells on the lower surface of the filter were fixed and stained with a Diff-Quick kit (Fisher Scientific, Waltham, MA) and photographed (magnification,  $\times 200$ ). Invasiveness was determined by counting cells in five microscopic fields per well, and the extent of invasion was expressed as an average number of cells per microscopic field. Cells were imaged with by phase-contrast microscopy (Leica Microsystems, Bannockburn, IL)

**Methylation-Specific Polymerase Chain Reaction.** DNA methylation was measured by the methylation-specific polymerase chain reaction (PCR) with genomic DNA (gDNA) incubated with sodium bisulfite using the EZ DNA Methylation-Direct kit (Zymo Research) by following the manufacturer's protocol. Primers used are listed in [Supporting Table 3](#) as indicated.

**Methylation-Specific Quantitative PCR.** We designed methylation-specific real-time qPCR primers

for CpG-rich regions using Methyl Primer Express v1.0 software (Applied Biosystems, Foster City, CA; [Supporting Table 4](#)). Quantification of DNA methylation status was determined using the EpiTect Methyl qPCR assay (SABiosciences, Frederick, MD) by following the manufacturer's protocol. Briefly, gDNA was digested with a combination of methylation-sensitive, methylation-dependent, both methylation-sensitive and methylation-dependent enzymes, or without enzyme added (mock) at 37°C for 16 hours. After enzyme inactivation at 65°C for 20 minutes, real-time qPCR was carried out according to the EpiTect protocol. All reactions were performed in triplicate. Relative fractions of methylated and unmethylated DNA were measured by comparing the amount in each digest with that of the mock digest using the  $\Delta$ Ct method.

**Quantification of 5hmC Levels in gDNA by Methylation-Sensitive qPCR.** gDNA was incubated with T4 Phage  $\beta$ -glucosyltransferase (New England Biolabs, Ipswich, MA) by following the manufacturer's protocol. First, 100 ng of glucosylated gDNA was digested with HpaII, MspI, or without enzyme (mock) at 37°C overnight and then incubated for 20 minutes at 80°C for enzyme deactivation. HpaII- or MspI-resistant DNA fraction was quantified by qPCR and normalizing to the mock control. MspI-resistant DNA represents the 5hmC DNA fraction, whereas the fraction of 5mC DNA was calculated by subtracting the 5hmC fraction from the resistance to HpaII. Primers were listed in [Supporting Table 5](#) as indicated.

**Liver Xenografts.** Six- to eight-week-old male BALB/c AnN nude mice were used for this experiment. SNU449-Luc cells were SNU449 cells labeled with firefly luciferase. First,  $2 \times 10^6$  SNU449-Luc cells stably transduced with miRZip-494 (anti-miR-494) or anti-miR control vector were injected orthotopically into liver of each nude mouse. For bioluminescent imaging, mice were anesthetized and then intraperitoneally injected with 150  $\mu$ g of D-luciferin per gram of body weight. *In vivo* tumor growth monitoring and *ex vivo* imaging of lung was carried out using IVIS 100 Imaging System (Xenogen, Hopkinton, MA).

## Results

**Identification of Differentially Regulated miRNAs Associated With HCC Invasion.** HCC often presents with multiple tumors, with only approximately 25% of tumors originating from *de novo* lesions.<sup>20</sup> Despite the observation that up to 75% of HCC tumor nodules within a given patient's liver are clonally related, the precise genomic profiles, and

therefore likely the phenotypes, are different among multifocal tumors. This within-patient tumor heterogeneity complicates HCC biomarker discovery and analysis, suggesting that biological drivers be considered on a tumor nodule basis, as opposed to an overall patient basis.<sup>21</sup>

Accordingly, we performed histological examination on all of the tumor nodules from each patient in a clinical cohort of HCC patients to identify those patients with and without vascular-invasive tumor nodules (Fig. 1A). As expected, HCC patients with vascular-invasive tumor(s) had significantly lower recurrence/metastasis-free survival rates than those without vascular-invasive tumors (Fig. 1B), reaffirming the fact that vascular invasion is an important predictor for HCC recurrence/metastasis.

In order to identify the potential deregulated miRNAs driving primary HCC tumors toward vascular invasiveness/metastasis, we subdivided each tumor into one of two groups: vascular invasion present (VI<sup>+</sup>) and vascular invasion absent (VI<sup>-</sup>). We then performed miRNA expression analysis using Affymetrix microarrays.

The first batch of 57 HCC tumors, as a pilot study, was analyzed and the differentially expressed miRNAs were obtained between 34 VI<sup>-</sup> and 23 VI<sup>+</sup> tumors. To avoid the potential batch effect, the second batch of 115 HCC tumor nodules included 57 VI<sup>-</sup> and 58 VI<sup>+</sup> tumors were then independently analyzed. We also applied miRNA obtained from five human HCC cell lines (HepG2, Hep3B, SNU398, SNU423, and SNU449) with either low or high invasion capabilities (Supporting Fig. 1) to miRNA microarray analysis in order to aid in clinical HCC vascular invasion miRNA discovery.

The differentially expressed miRNAs of all three data sets were identified and summarized (Supporting Table 1), and two distinctive expression clusters of miRNAs were obtained by supervised hierarchical clustering analysis in each data set (Fig. 1C-E). Moreover, unsupervised clustering analyses confirmed that the differentially expressed miRNAs can mostly discriminate VI<sup>+</sup> and VI<sup>-</sup> tumors (Supporting Fig. 2). We further examined the overlap between the three lists of differentially expressed miRNAs (VI<sup>+</sup> vs. VI<sup>-</sup>) and found that 47 down-regulated miRNAs and 20 up-regulated miRNAs were similarly altered in all three data sets (Fig. 1F; Table 1); these sets of commonly differentially expressed miRNAs were statistically significant ( $P < 10^{-25}$ ). Within 47 down-regulated miRNAs, most had been previously reported as tumor-suppressor miRNAs, such as let-7g, miR-15a, miR-16, miR-29 family, miR-34a, miR-99a, miR-100, miR-

122, miR-126, miR-143, miR-146, miR-148a, miR-152, miR-192, miR-194, miR-195, miR-497, and the miR-200 family.

Among the shared 20 significantly up-regulated miRNAs in VI<sup>+</sup> HCC tumors and high-invasive HCC cell lines, we focused on miR-494 because it exhibited the highest up-regulated fold change in all of the three microarray data sets (Supporting Table 1; Supporting Fig. 3). To further address the relationship between tumor miR-494 levels and recurrence-free survival rates of HCC patients, we analyzed miR-494 expression levels in all 172 HCC tumors by real-time quantitative PCR (qRT-PCR). We showed that miR-494 qRT-PCR results are highly associated with microarray data sets (Supporting Fig. 4). All tumors were further classified into two groups based on low (miR-494<sup>low</sup>) and high miR-494 expression (miR-494<sup>high</sup>) with median division of all samples (Supporting Fig. 5). Strikingly, HCC patients carrying at least one miR-494<sup>high</sup> tumor nodule had poor survival rates, as compared to those who only had miR-494<sup>low</sup> tumor(s) (Fig. 1G). Moreover, Cox's proportional hazards regression analysis (Supporting Table 2) demonstrated that tumor miR-494 expression level is an independent predictor for HCC recurrence.

Notably, it has been shown that miR-494 may act as a convergent hub for upstream oncogenic transcriptional factors, such as H-Ras, c-Jun, c-Fos, and E2F family.<sup>22,23</sup> Recently, it has also been shown that overexpression of Myc and Ras up-regulates miR-494 expression, which then subsequently promotes HCC cell proliferation through accelerating G<sub>1</sub>/S transition.<sup>22</sup> Having demonstrated that miR-494 is abundant in high-invasive (SNU423 and SNU449), but not low-invasive, HCC cell lines (HepG2, Hep3B, and SNU398; Fig. 1E), we next sought to evaluate whether miR-494 can increase the invasion ability of HCC cells.

**miR-494 Triggers HCC Cell Migration/Invasion.** To investigate whether miR-494 alters HCC cell migration/invasion ability, we transduced a lentiviral vector harboring the human miR-494 gene into low-invasive cell lines HepG2, Hep3B, and SNU398. We found that ectopic expression of miR-494 leads to increased cell motility in both cell migration and invasion assay (Fig. 2A-C). Our results show that cells with enforced expression of miR-494 had diminished expression of epithelial marker E-cadherin and a robust induction of the mesenchymal markers, N-cadherin, vimentin, fibronectin, zinc-finger E-box binding homeobox (ZEB)1, and ZEB2, with a decrease of E-cadherin (Fig. 2D). The E-box-binding



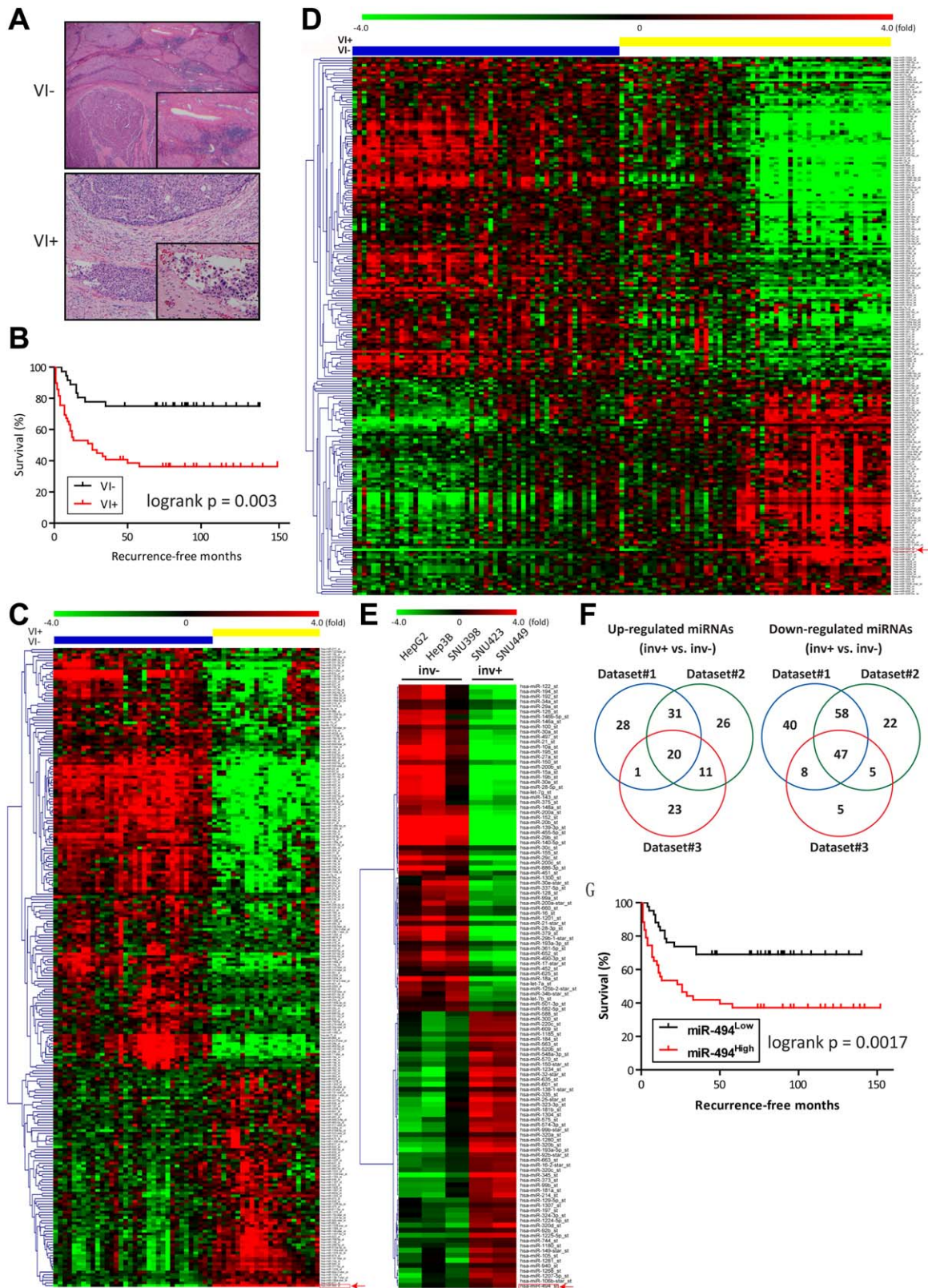


Fig. 1. miR-494, associated with poor clinical outcome, is the most up-regulated miRNA in invasive human HCC tumors and cell lines. (A) Representative photomicrographs of human HCC without and with vascular invasion. Left panel, HCC tumor capsule without vascular invasion. Right panel, HCC tumor with vascular invasion. (B) Kaplan-Meier's plot shows recurrence-free survival of patients who carried at least 1 tumor with vascular invasion, and that of those patients who only carried tumor(s) without vascular invasion. Total HCC patient numbers are 86. (C, D, and E) Hierarchical clustering of differentially expressed miRNAs. miR-494 is indicated by an arrowhead. (C) Data set 1 includes 23 human HCC tumors with vascular invasion (yellow bars) and 34 tumors without vascular invasion (blue bars). (D) Data set 2 includes 58 human HCC tumors with vascular invasion (yellow bars) and 57 tumors without vascular invasion (blue bars). (E) Data set 3 includes two high-invasive human HCC cell lines (SNU423 and SNU449) and three low-invasive cell lines (HepG2, Hep3B, and SNU398). (F) Venn diagram identifies overlapped differentially expressed miRNAs among data sets 1, 2, and 3. (G) Kaplan-Meier's plot represents recurrence-free survival of HCC patients who carried at least 1 tumor with high expression of miR-494 and that of those patients who only carried tumor(s) with low miR-494 expression. Total HCC patient numbers are 86.

**Table 1. Overlap Between Three Lists of Differentially Expressed miRNAs**

Differentially Regulated miRNAs Shown in all Three Databases		
Down-regulated miRNAs (inv <sup>+</sup> vs. inv <sup>-</sup> )	Up-regulated miRNAs (inv <sup>+</sup> vs. inv <sup>-</sup> )	
hsa-miR-122_st	hsa-miR-200a_st	hsa-miR-494_st
hsa-miR-194_st	hsa-miR-152_st	hsa-miR-1207-5p_st
hsa-miR-192_st	hsa-miR-20b_st	hsa-miR-1268_st
hsa-miR-34a_st	hsa-miR-455-5p_st	hsa-miR-940_st
hsa-miR-29a_st	hsa-miR-29b_st	hsa-miR-1281_st
hsa-miR-126_st	hsa-miR-140-5p_st	hsa-miR-149-star_st
hsa-miR-146b-5p_st	hsa-miR-30c_st	hsa-miR-1180_st
hsa-miR-146a_st	hsa-miR-155_st	hsa-miR-744_st
hsa-miR-100_st	hsa-miR-29c_st	hsa-miR-1225-5p_st
hsa-miR-30a_st	hsa-miR-200c_st	hsa-miR-320d_st
hsa-miR-497_st	hsa-miR-451_st	hsa-miR-1224-5p_st
hsa-miR-21_st	hsa-miR-337-5p_st	hsa-miR-1307_st
hsa-miR-10a_st	hsa-miR-128_st	hsa-miR-663_st
hsa-miR-195_st	hsa-miR-99a_st	hsa-miR-92b-star_st
hsa-miR-27a_st	hsa-miR-660_st	hsa-miR-575_st
hsa-miR-150_st	hsa-miR-16_st	hsa-miR-25-star_st
hsa-miR-200b_st	hsa-miR-21-star_st	hsa-miR-138-1-star_st
hsa-miR-15a_st	hsa-miR-28-3p_st	hsa-miR-635_st
hsa-miR-19b_st	hsa-miR-379_st	hsa-miR-1234_st
hsa-miR-30e_st	hsa-miR-193a-3p_st	hsa-miR-150-star_st
hsa-miR-28-5p_st	hsa-miR-361-5p_st	
hsa-let-7g_st	hsa-miR-17-star_st	
hsa-miR-143_st	hsa-miR-18a_st	
hsa-miR-148a_st		

transcription factors, ZEB1 and ZEB2, are the transcriptional repressors for E-cadherin and have been shown to trigger epithelial-mesenchymal transition (EMT) in cancers.<sup>24</sup> Therefore, our results implicate that miR-494-transduced cells might be undergoing EMT, which is recognized as a critical reprogramming step driving tumor invasion and metastasis.

**miR-494 Inactivates Gene Transcription of Multiple Invasion-Suppressor miRNAs.** We then investigated whether miR-494 could alter other miRNAs relevant to tumor invasion. It was observed that the ectopic expression of miR-494 can repress the transcription of multiple invasion-suppressor miRNAs, including miR-126, miR-148a, miR-152, miR-192, miR-194, miR-195, miR-497, and the miR-200 family (Fig. 2E). These miRNAs were down-regulated in invasive HCC tumors and cell lines in all of the three independent microarray data sets (Fig. 1B-D), and they could retard invasion ability, as compared to the negative control (Supporting Fig. 6; Supporting References).

Specifically, the miR-200 family and miR-192 are known as important regulators of EMT through directly targeting of ZEB1 and ZEB2 mRNAs.<sup>25-27</sup> We found that miR-494 is able to suppress expression levels of miR-200 family members and miR-192 (Fig. 2E), which may lead to tumor EMT by increasing

expression of ZEB1, ZEB2, N-cadherin, vimentin, and fibronectin (Fig. 2D). These data suggest that miR-494 might promote EMT by down-regulating miR-200 family members and miR-192 in HCC cells.

**miR-494 Triggers Gene Silencing of Multiple Invasion-Suppressor miRNAs by Inhibiting gDNA Demethylation.** It has been recently reported that CpG island hypermethylation-induced epigenetic repression of the miR-200 family leads to up-regulation of ZEB1 and ZEB2 expression, and this is correlated with increased EMT and metastasis.<sup>28-30</sup> Therefore, we therefore analyzed the proximal CpG-rich regions of miR-126, miR-148a, miR-152, miR-192, miR-194, miR-195, miR-497, and miR-200 family genes using the methyl-specific PCR and qPCR analyses. Our data indicate that they are hypermethylated upon miR-494 overexpression (Fig. 2F,G), and bioinformatics analysis also suggests that CpG islands do exist in the regulatory sequences of those miRNA genes (Table 2; Supporting Fig. 7).

Furthermore, we found that a DNA-demethylating agent, 5'-aza-2'-deoxycytidine (5'-Aza), was able to diminish the inhibitory effects of miR-494 on expression of multiple invasion-suppressor miRNAs (Fig. 2H), suggesting that miR-494 can regulate multiple invasion-suppressor miRNAs through controlling gDNA methylation status.

5hmC has been demonstrated to be a novel demethylation marker associated with cancer progression.<sup>17,18,31</sup> Therefore, we next investigate whether miR-494 could inhibit gene expression of multiple invasion-suppressor miRNAs by altering genomic 5hmC levels. Our results show that enforced expression of miR-494 remarkably abolished 5hmC levels in proximal CpG island regions of multiple invasion-suppressor miRNA genes (Fig. 2I). Collectively, these results suggest that miR-494 can block DNA demethylation in proximal CpG islands of multiple invasion-suppressor miRNAs and inhibit their expression, resulting in an up-regulation of their downstream targets.

**miR-494 Regulates 5-hmC Level by Targeting TET Methylcytosine Dioxygenase.** Next, we analyzed potential gene targets of miR-494 by prediction algorithms, including DIANA-microT (<http://diana.imis.athena-innovation.gr/DianaTools/index.php>), miRanda (<http://www.microrna.org/>), miRBase (<http://www.mirbase.org/>), miRDB (<http://mirdb.org/miRDB/>), miR-Walk (<http://www.umm.uni-heidelberg.de/apps/zmf/mirwalk/>), PicTar (<http://pictar.mdc-berlin.de/>), TargetScan (<http://www.targetscan.org/>), and EIMMO (<http://www.mirz.unibas.ch/EIMMO2>).



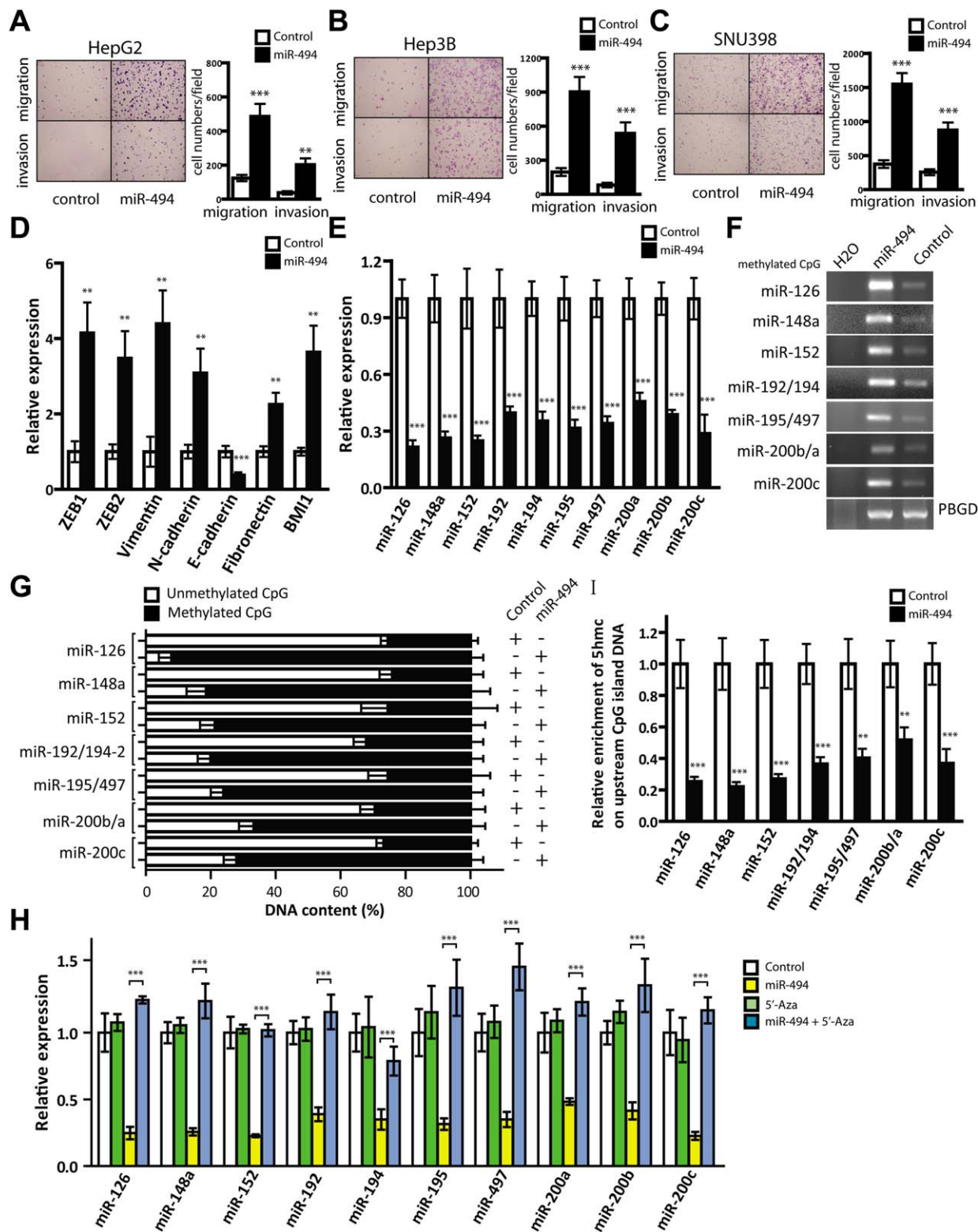


Fig. 2. miR-494 promotes HCC cell migration/invasion and suppresses multiple invasion-suppressor microRNAs by inhibiting DNA demethylation of their proximal CpG islands. (A, B, and C) (A) HepG2 cells, (B) Hep3B cells, or (C) SNU398 cells, transduced with miR-494 or the nontarget control vector, were subjected to cell migration and invasion assays. Migrated/invaded cells in fields were quantified and representative photographs are shown. Data are represented as mean  $\pm$  standard deviation (SD) from four independent experiments. (D and E) qRT-PCR analysis of RNAs from HepG2 cells transduced with miR-494-expressing vector or the nontarget control vector for (D) indicated biomarkers of EMT and (E) indicated microRNAs. (F) Methylation-specific PCR analysis of the proximal CpG island regions of the indicated miRNA genes with gDNAs purified from HepG2 cells transduced with the miR-494 expression vector. PBGD served as the control. (G) DNA methylation status of the proximal CpG regions of the indicated miRNA genes in HepG2 cells transduced with either miR-494-expressing vector or the nontarget control vector. DNA methylation status was determined using methylation-sensitive/dependent restriction digestion followed by qRT-PCR analysis. Data are represented as mean  $\pm$  SD from three independent experiments. (H) Restored expression of miR-200c upon adding DNA demethylating agent 5'-Aza in HepG2 cells transduced with the miR-494-expressing vector. Data are represented as mean  $\pm$  SD from five independent experiments. (I) GlucMS-qPCR analysis of proximal CpG islands within the indicated miRNA gene's upstream regions enriched for 5hmC in HepG2 cells transduced with the miR-494-expressing vector. Data are represented as mean  $\pm$  SD from five independent experiments. \*\* $P$  < 0.01; \*\*\* $P$  < 0.001. Abbreviation: PBGD, porphobilinogen deaminase.

**Table 2. gDNA Sequences Surrounding the Indicated miRNA Genes Were Analyzed for CpG Islands (CGIs) Using UCSC Genome Browser Analysis.**

MicroRNA	Accession	Chromosome	Strand	CGI distance to Pre-miRNA 5' End	CGI No. (Distance <3 kb)	CGI No. (Distance <10 kb)
hsa-miR-494	MI0003134	14	+	146111	0	0
hsa-miR-126	MI0000471	9	+	54, 4049	1	2
hsa-miR-148a	MI0000253	7	-	407	1	1
hsa-miR-152	MI0000462	17	-	47	1	1
hsa-miR-192	MI0000234	11	-	3745	0	1
hsa-miR-194-2	MI0000732	11	-	3552	0	1
hsa-miR-195	MI0000489	17	-	4381	0	1
hsa-miR-497	MI0003138	17	-	4060	0	1
hsa-miR-200a	MI0000737	1	+	2659, 9767	1	2
hsa-miR-200b	MI0000342	1	+	1900, 9008	1	2
hsa-miR-200c	MI0000650	12	+	6572	0	1

Abbreviations: UCSC, University of California Santa Cruz; CGI, CpG island; kb, kilobases.

Most notably, among the predicted targets (Fig. 3A) are TET methylcytosine dioxygenases, which are able to trigger global DNA demethylation by converting 5mC to 5hmC. Recently, TET methylcytosine dioxygenases have been reported to play an important role in epigenetic reprogramming, cell differentiation, and cancer progression.<sup>14-16,32</sup>

We then sought to examine expression levels of three TET methylcytosine dioxygenases in five human HCC cell lines. Our results show that TET1 is the most abundant isoform in HCC cells and is much more abundant than TET2; in contrast, TET3 is hardly detectable in HCC cell lines (Fig. 3B). More important, we found that expression levels of TET methylcytosine dioxygenases are remarkably higher in low-invasive cells (HepG2, Hep3B, and SNU398) than that in high-invasive HCC cells (SNU423 and SNU498), indicating that gene expression of TET methylcytosine dioxygenases are inversely associated with miR-494 level and HCC cell invasive ability.

Because all three of the TET isozymes are the predicted targets of miR-494, we next evaluated whether miR-494 can actually regulate their gene expression. Our results revealed that miR-494 overexpression in HepG2 and Hep3B cells results in a significant down-regulation of TET1, TET2, and TET3 genes (Figs. 3C and Supporting Fig. 8), whereas inhibition of miR-494 in SNU449 and SNU423 cells leads to increasing their expression levels (Figs. 3D and Supporting Fig. 9). In addition, our data also demonstrated that miR-494 overexpression leads to a down-regulation of a few high-scoring predicted miR-494 targets (Supporting Fig. 10), such as mutated in colorectal cancer (MCC), Rho-associated, coiled-coil containing protein kinase 1, phosphatase and tensin homolog (PTEN), fibroblast growth factor receptor 2, and leukemia inhibitory factor, consistent with the previous findings in the literature.<sup>22,33</sup>

Because TET1 is the predominant isoform among three TET isozymes in HCC cells (Fig. 3B) and there are highly predicted miR-494 targeting positions found in the 3' untranslated region (UTR) region of the TET1 gene (Fig. 3E), we next sought to explore whether there is a direct interaction between miR-494 and the TET1 gene. To this end, we performed a luciferase reporter assay using the 3' UTR region of TET1 (Fig. 3F) and its mutant in the miR-494 recognition site. Our data demonstrate that miR-494 is able to suppress TET1 gene expression by targeting its 3' UTR region (Fig. 3F).

It has been recently revealed that 5hmC levels decrease in cells upon inhibition of TET methylcytosine dioxygenase.<sup>17,18,31</sup> Therefore, we next investigated the ability of miR-494 to alter 5hmC levels in human gDNA by TET methylcytosine dioxygenase with a dot blot assay using anti-5hmC antibodies. The result demonstrated that ectopic expression of miR-494 can reduce global 5hmC levels in gDNA (Fig. 3G), implicating that alteration of DNA demethylation status may account for the effect of miR-494 to promote HCC tumor invasion.

**Inhibition of miR-494 or TET1 Alters Gene Expression Levels of Multiple Invasion-Suppressor miRNAs and Tumor Cell Invasion.** The findings that ectopic expression of miR-494 promotes HCC cell invasion and inhibits TET methylcytosine dioxygenase and multiple invasion-suppressor miRNAs led us to further explore whether miR-494 inhibition could inhibit tumor cell invasion. If so, we posited that this would be affected through restoring transcriptional activation of multiple invasion-suppressor miRNAs caused by the resurrection of TET methylcytosine dioxygenase, especially TET1.

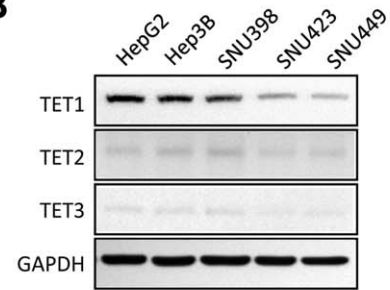
To investigate the consequences of miR-494 inhibition, we transduced high-invasive SNU449 cells (which



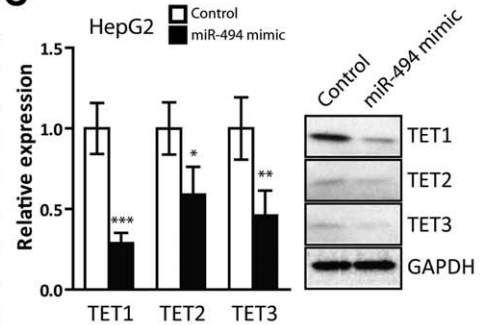
**A**

Gene	DIANAmT	miRanda	miRDB	miRWalk	PICTAR5	Targetscan	EIMMO	Score
TET1	1	1	1	1	1	1	1	7
FGFR2	1	1	1	1	1	1	1	7
ROCK1	1	1	1	1	1	1	1	7
IGF2BP1	1	1	1	1	1	1	1	7
LIF	1	1	0	1	1	1	1	6
PTEN	1	1	1	1	1	1	0	6
CFTR	1	1	1	0	1	1	1	6
BIRC5	1	1	0	1	1	1	1	6
SLC12A2	1	1	0	1	1	1	1	6
MCC	0	1	0	1	1	1	1	5
FBN2	1	1	0	1	1	1	0	5
CDK6	1	0	1	1	1	1	0	5
TET2	1	1	0	1	0	1	0	4
TET3	0	1	0	0	1	1	1	4
RUNX1	1	0	0	1	1	1	0	4
JUN	1	1	0	0	1	1	0	4

**B**



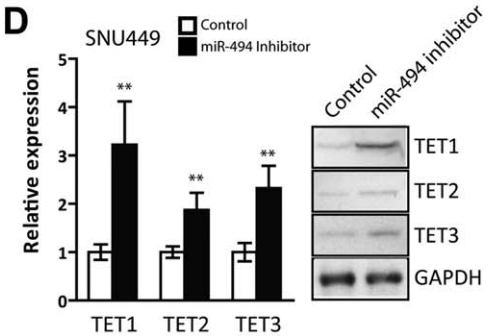
**C**



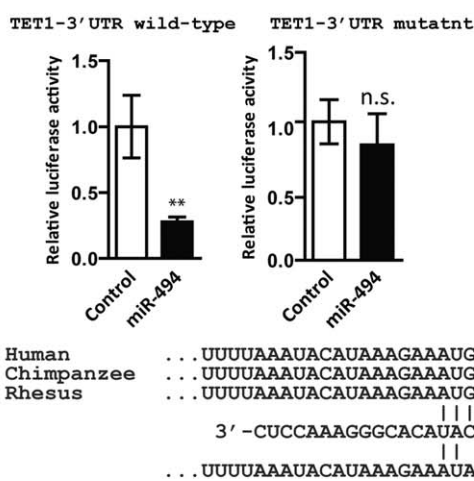
**E**

	pairing of target region and miRNA	seed match
Position 242-248 of TET1 3' UTR	5' . . . UAAAUACAUAAGAAAUGUUUCA . . . hsa-miR-494 3' CUCCAAGGGCACAUCAAAGU	8mer
Position 1432-1438 of TET1 3' UTR	5' . . . GAUUACCCAAACAACAUUUUCG . . . hsa-miR-494 3' CUCCAAGGGCACAUCAAAGU	7mer
Position 2401-2407 of TET1 3' UTR	5' . . . AUAGUAUCAACUGAAAUGUUUCC . . . hsa-miR-494 3' CUCCAAGGGCACAUCAAAGU	7mer

**D**



**F**



**G**

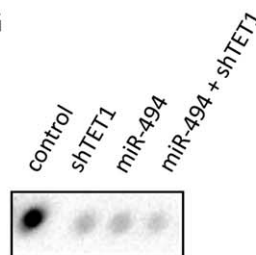


Fig. 3. miR-494 triggers gene inactivation of multiple invasion-suppressor microRNAs by targeting TET methylcytosine dioxygenase. (A) A list of selected high-scoring predicted miR-494 targets was produced by various programs using different algorithms. (B) Cell lysates isolated from five HCC cell lines were subjected to western blotting analysis for TET1, TET2, and TET3 proteins. (C and D) Total RNAs or cell lysates isolated from HepG2 cells transfected with miR-494 mimic or (C) SNU449 cells transfected with miR-494 inhibitor (D) were subjected to qRT-PCR or western blotting analysis for TET1, TET2, and TET3 mRNA. Data are represented as mean  $\pm$  standard deviation (SD) from five independent experiments. (E) Putative binding sites of miR-494 in TET1 3' UTR. Predicted 8- or 7-mer binding seeds of miR-494 to TET1 3' UTR are indicated with vertical lines. (F) Luciferase assay of the *TET1* 3' UTR luciferase plasmid. CV-1 cells were transiently cotransfected with the wild-type or miR-494-binding mutant of human *TET1* 3' UTR luciferase plasmid with *Renilla* luciferase reporter for normalization. Data are represented as mean  $\pm$  SD from four independent experiments. Putative miR-494-binding site on the 242-248 base-pair region of TET1 3' UTR was mutated as indicated. (G) gDNA purified from HepG2 cells transfected with miR-494 or TET1 short hairpin RNA-expressing vector or the negative control was denatured and neutralized. Global 5hmC levels were then determined using a dot blot assay with anti-5hmC antibody. \* $P$  < 0.05; \*\* $P$  < 0.01; \*\*\* $P$  < 0.001. Abbreviations: GAPDH, glyceraldehyde 3-phosphate dehydrogenase; n.s., not significant.

express abundant levels of endogenous miR-494) with either a control or miRZip antisense miR-494-encoded lentivirus. MiR-494 inhibition by anti-miR-494 in SNU449 cells resulted in a significant inhibition of cell migration/invasion (Fig. 4A,B). Also noted in this experiment were reduction in protein expression of the mesenchymal biomarker, vimentin (Fig. 4C) and a dramatic increase in expression of multiple invasion-suppressor miRNAs (Fig. 4D). We were next interested whether inhibition of TET1 gene expression contributes to HCC cell invasion triggered by miR-494. Interestingly, knockdown of TET1 alone in HepG2 cells by using RNA interference (RNAi) can promote HCC cell migration/invasion similar to the effect of miR-494 transduction (Fig. 4E,F), implicating TET1 might play a key role in miR-494-mediated HCC migration/invasion. Furthermore, we also found that knockdown of TET1 led to down-regulation of multiple invasion-suppressor miRNAs. This was caused by the decrease of 5hmC levels on their gene promoter/enhancer (Fig. 4G,H), suggesting that TET1 may also be involved in miR-494-mediated transcriptional repression of multiple invasion-suppressor miRNAs.

**miR-494 Targeting on TET1 Led to Down-Regulation of Multiple Invasion-Suppressor miRNAs and HCC Cell Invasion.** To investigate whether TET1 overexpression could abolish miR-494-mediated HCC cell invasion, we transfected a TET1-expressing plasmid into SNU449 or HepG2 cells and then performed cell migration/invasion assays. Notably, overexpressed TET1, but not kinase-dead TET1 mutant, dramatically decreased cell migration/invasion ability promoted by miR-494 (Fig. 5A-C). In addition, overexpression of TET1 can rescue repression of multiple invasion-suppressor miRNAs and the reduced global 5hmC level elicited by miR-494 overexpression (Fig. 5D,E). Our results suggest that TET enzymes, especially TET1, can suppress HCC cell invasion by up-regulating multiple invasion-suppressor miRNAs by demethylating gDNA.

To determine whether cell invasion inhibition triggered by miR-494 inhibition is a result of TET1, we transduced HCC cells with anti-miR-494 and then knocked down TET1 by RNAi in invasive SNU449 cells (Fig. 5F). Inhibition of cell invasion by anti-miR-494 can be rescued by TET1 knockdown (Fig. 5G).

We further investigated whether miR-494 expression was associated with EMT and inversely correlated with 5hmC level and TET1 expression in clinical HCC tumor specimens. Immunohistochemical analyses revealed distinct expression patterns of vimentin, E-cadherin, 5hmC, and TET1 between miR-494<sup>low</sup>

and the miR-494<sup>high</sup> tumors. MiR-494<sup>high</sup> tumors have significantly higher frequency of VI (Fig. 6A,B), higher level of vimentin, and lower levels of 5hmC and TET1 (Fig. 6C), whereas higher protein level of E-cadherin was mostly found in miR-494<sup>low</sup> tumors. These results are consistent with our *in vitro* findings that miR-494 can trigger HCC cell invasion by targeting TET1 and suppressing gDNA demethylation.

We then investigated the impact of miR-494 inhibition on HCC metastasis *in vivo* using an orthotopic HCC xenograft model. Stably miR-494 knocked down SNU449-Luc cells were implanted into livers of nude mice. We observed that miR-494 inhibition reduced the ability of implanted cells to form tumors (Fig. 6D), which is consistent with a finding that miR-494 inhibition can inhibit HCC cell growth.<sup>22</sup> More important, miR-494 inhibition significantly abolished lung metastasis, as shown by bioluminescent imaging (Fig. 6E), suggesting that miR-494 promotes HCC metastasis.

Collectively, our data suggest that TET1 is a direct target of miR-494 and its down-regulation by miR-494 is responsible for gene inactivation of multiple invasion-suppressor miRNAs and HCC invasion/metastasis (Fig. 6F).

## Discussion

A few studies have shown that miR-494 may increase proliferation activity in HCC cells and apoptosis resistance in H460 human lung cancer cells.<sup>22,34</sup> In addition, miR-494 was found to target specific tumor-suppressor genes, such as *MCC* and *PTEN*.<sup>22,35</sup> However, paradoxically, miR-494 has also been reported to inhibit cell growth in A549 human lung cancer cells, cholangiocarcinoma, and SMAD4-deficient pancreatic ductal adenocarcinoma.<sup>36-38</sup> It has been well known that miRNAs would exhibit cell-type or tissue-specific actions in a context-dependent manner, which may explain the differences between those studies.

Here, we demonstrate that miR-494 triggers gene inactivation of multiple invasion-suppressor miRNAs through direct targeting of TET methylcytosine dioxygenase. This results in DNA hypermethylation in the proximal CpG regions of multiple invasion-suppressor miRNA genes, which eventually leads to HCC tumor vascular invasion. The demethylating agent 5'-Aza is able to rescue miR-494-mediated suppression of multiple invasion-suppressor miRNAs and block *in vitro* cell invasion ability (Fig. 2H). These observations suggest that DNA methylation/demethylation is a key mechanism of regulating multiple invasion-suppressor miRNAs and controlling tumor vascular invasion.

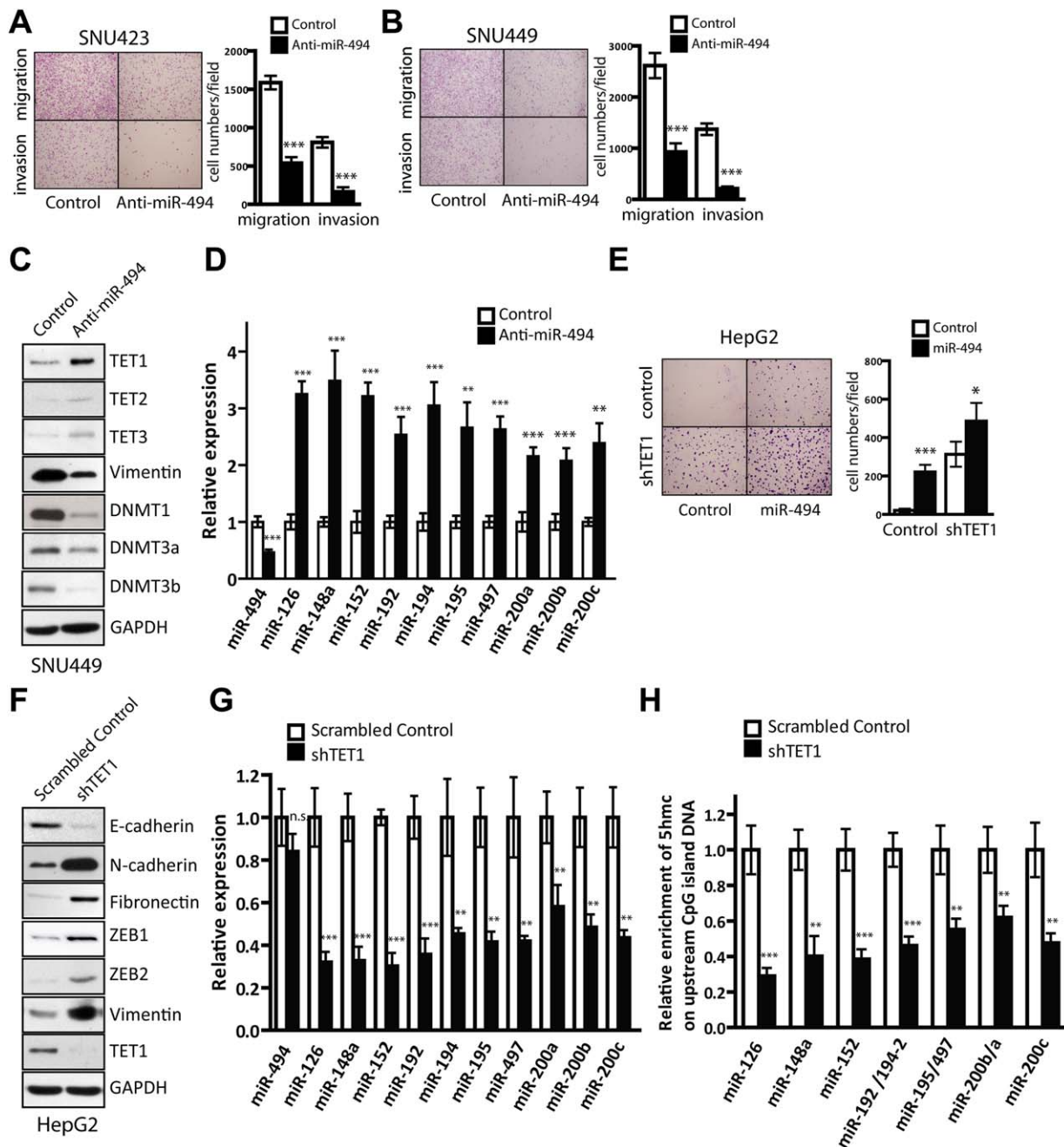


Fig. 4. Knockdown of miR-494 or TET1 impacts on HCC cell invasion ability and expression of multiple invasion-suppressor miRNAs. (A and B) (A) SNU449 cells or (B) SNU423 cells, stably transduced with anti-miR-494 or anti-miR control vector, were subjected to cell migration and invasion assays. Migrated/invaded cells in fields were quantified and representative photographs are shown. Data are represented as mean  $\pm$  standard deviation (SD) from four independent experiments. (C) Cell lysates from SNU449 cells, stably transduced with anti-miR-494 expressing vector or anti-miR control vector, were subjected to western blotting analysis for the indicated proteins. (D) qRT-PCR analysis of the indicated miRNAs with total RNAs from SNU449 cells transduced with anti-miR-494 or anti-miR control. Data are represented as mean  $\pm$  SD from five independent experiments. (E) HepG2 cells transduced with the combination of miR-494, TET1 short hairpin RNA (shRNA) or the control vectors were subjected to the cell migration assay and then migrated cells were quantified. Data are represented as mean  $\pm$  SD from four independent experiments. (F) Cell lysates from HepG2 cells transduced with TET1 shRNA or the scrambled control vector were subjected to western blotting analysis for the indicated proteins. (G) qRT-PCR analysis of invasion-suppressor miRNAs with total RNAs isolated from HepG2 transduced with TET1 short hairpin RNA (shRNA) and the scrambled control. Data are represented as mean  $\pm$  SD from five independent experiments. \* $P < 0.05$ ; \*\* $P < 0.01$ ; \*\*\* $P < 0.001$ . (H) GlucMS-qPCR analysis of CpG islands within the indicated multiple invasion-suppressor miRNA genes' upstream regions specifically enriched for 5hmC in HepG2 cells infected with TET1 shRNA and control vectors. Data are represented as mean  $\pm$  SD from three independent experiments. Abbreviations: GAPDH, glyceraldehyde 3-phosphate dehydrogenase; n.s., not significant.



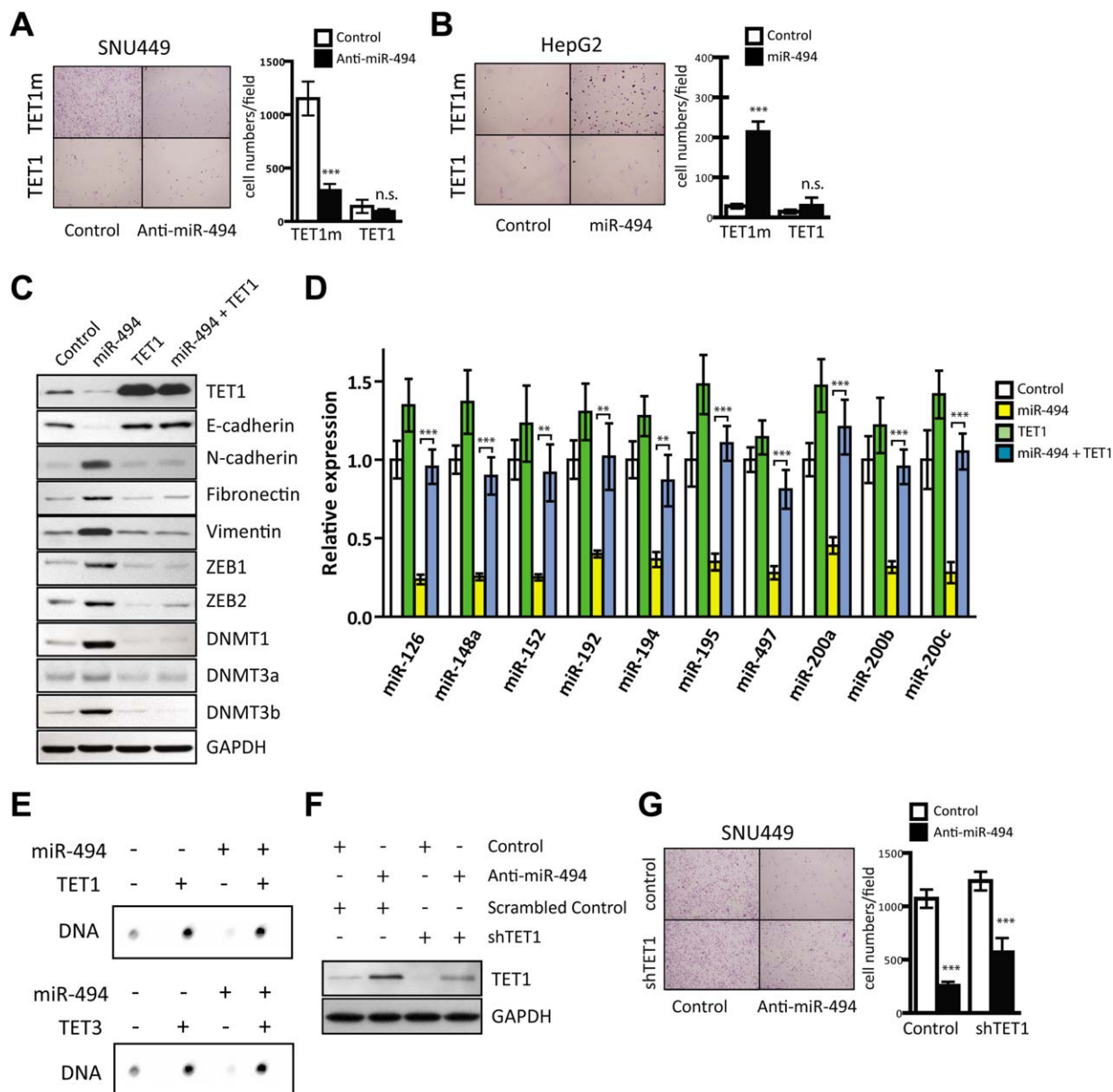


Fig. 5. TET methylcytosine dioxygenase is essential for inhibition of miR-494-mediated HCC invasion/EMT and suppression of multiple invasion-suppressor miRNAs. (A) SNU449 cells transduced with the combination of anti-miR-494, TET1 (wild-type), or negative controls (anti-miR control and catalytic-dead TET1m mutant) and (B) HepG2 cells transduced with the combination of miR-494, TET1, or negative controls (anti-miR control and catalytic-dead TET1m mutant) were subjected to cell invasion assay. Migrated cells in fields were quantified and representative photographs are shown. Data are represented as mean  $\pm$  standard deviation (SD) from four independent experiments. (C) Cell lysates from HepG2 cells infected with the combination of the miR-494 with TET1 or the control vector were subjected to western blotting for the indicated proteins. (D) qRT-PCR analysis of invasion-suppressor miRNAs with total RNAs isolated from HepG2 cells transduced with the combination of miR-494 with TET1 or the empty vector. Data are represented as mean  $\pm$  SD from five independent experiments. (E) gDNA isolated from HepG2 cells transduced with the combination of miR-494 with TET1 or TET3 expression vector was denatured and neutralized. 5hmC levels were determined by the dot blot assay using anti-5hmC antibody. (F and G) SNU449 cells expressing a combination of anti-miR-494 and the TET1 short hairpin RNA (shRNA) expression vector were subjected to either (F) western blotting analysis of TET1 or (G) cell invasion assay. Data are represented as mean  $\pm$  SD from five independent experiments. \* $P$  < 0.05; \*\* $P$  < 0.01; \*\*\* $P$  < 0.001. Abbreviations: GAPDH, glyceraldehyde 3-phosphate dehydrogenase; n.s., not significant.

Notably, miR-126, miR-148a, and miR-152 have been reported to reduce gDNA methylation by targeting DNA methyltransferases (DNMTs) 1 and 3b.<sup>39-43</sup> Therefore, it is reasonable to further hypothesize that miR-494 may increase DNMT1/DNMT3b expression

by down-regulating miR-126, miR-148a, and miR-152. Indeed, we observed that enforced expression of miR-494 increases DNMT1 and DNMT3b expression levels (Fig. 5C), whereas miR-494 inhibition suppresses them (Fig. 4C). These results suggest that miR-

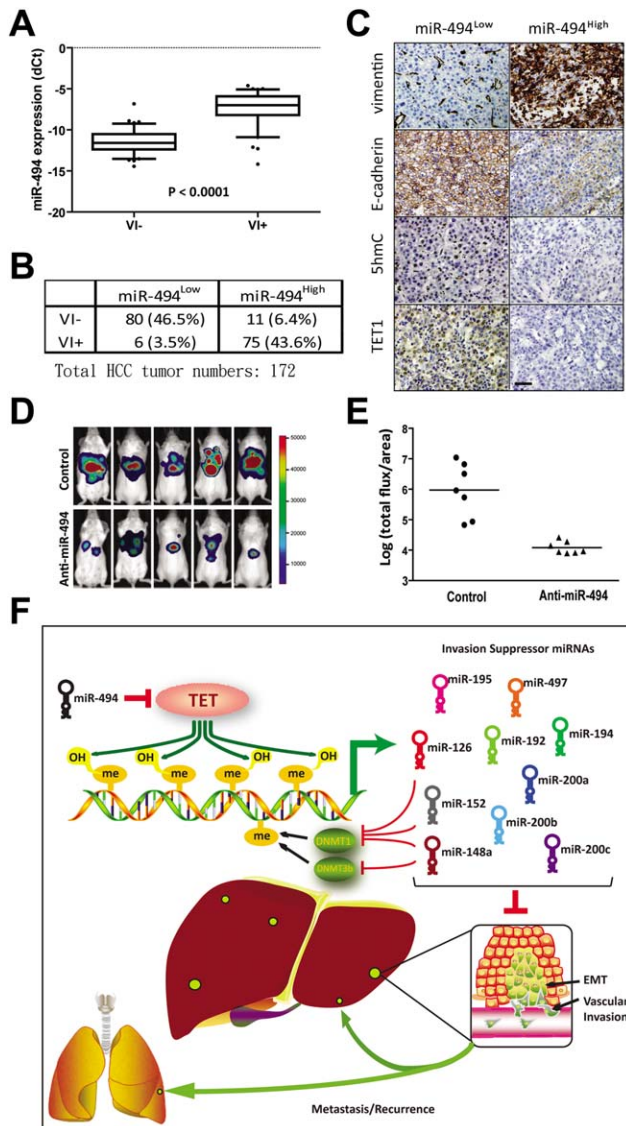


Fig. 6. miR-494 is associated with HCC EMT and vascular invasion in human HCC tumors. (A) Analysis of miR-494 expression of 91 VI<sup>-</sup> and 81 VI<sup>+</sup> HCC tumors by qRT-PCR. (B) Vascular invasion is associated with higher miR-494 levels in human HCC tumors. Human HCC tumor samples were classified into two groups according to low and high miR-494 expression levels by median division of qRT-PCR results. (C) Representative Images of immunohistochemical staining for vimentin, E-cadherin, 5hmC, and TET1 in HCC tumors with low (miR-494<sup>low</sup>) and high miR-494 (miR-494<sup>high</sup>) expression levels. Scale bars, 100  $\mu$ m. (D) Bioluminescent images showed a suppression of tumor formation in nude mice implanted with miR-494 knockdown SNU449-Luc cells ( $n = 5$  for each group). (E) Suppression of lung metastasis in nude mice implanted with miR-494 knockdown SNU449-Luc cells was monitored by *ex vivo* bioluminescent imaging. Luciferase activity of lung metastasis was quantified for anti-miR-494 or anti-miR control group ( $n = 7$  for each group). (F) Schematic presentation of miR-494 action in HCC EMT and vascular invasion. miR-494 suppresses multiple invasion-suppressor miRNAs through epigenetic repression by targeting TET methylcytosine dioxygenase in invasive human hepatocarcinoma tumors.

494 controls gDNA methylation/demethylation status not only by TET methylcytosine dioxygenase, but also by DNMTs.

Thus far, the distinct role of the TET family of methylcytosine dioxygenases in tumor development remains unclear, though it has been reported that depletion of TET1 and 5hmC has been observed in progression of solid tumors,<sup>17-19,44,45</sup> and TET2 mutations with reduced 5hmC levels were found to be associated with bone marrow malignancies.<sup>15,46</sup> A recent report has revealed that mutations of the isocitrate dehydrogenase (IDH) genes IDH1 and IDH2 result in deregulated production of 2-hydroxyglutarate, which can inactivate TET methylcytosine dioxygenase activity, leading to DNA hypermethylation in acute myeloid leukemia cells.<sup>47</sup> This finding further supports the notion that TET methylcytosine dioxygenase plays a key role in aberrant epigenetic regulation during cancer progression. In this study, we demonstrated that knockdown of the TET1 gene can promote HCC cell invasion, which is in agreement with a previous study showing that TET1 depletion enhances mammary and prostatic tumor invasion and metastasis.<sup>48</sup> Our results further demonstrate that miR-494-elicited HCC cell invasion can be diminished by enforced expression of TET1, implicating that TET1 may serve as a major gene target in mediating the effect of miR-494 in HCC cell invasion.

In this study, we reported that TET1 can activate multiple invasion-suppressor miRNA genes by DNA demethylation in their proximal CpG regions. A recent report has shown that in metastatic prostatic and mammary tumor cells, gene silencing of tissue inhibitors of metalloproteinases can be resurrected by TET1 overexpression by demethylating its gene promoter.<sup>48</sup> Whether there are more invasion-suppressor genes that can also be epigenetically activated by TET proteins during HCC tumor invasion is worthy of further investigation.

Liver cells have been shown to easily uptake oligonucleotides, as compared with other tissues,<sup>49</sup> implicating that miRNA inhibition or replacement might serve as a potential therapeutic approach against HCC invasion and metastasis.<sup>50</sup> Considering the safety issues over the clinical application of retroviral or adeno-associated virus vector-based gene therapy, the use of miRNA antagonists to inactivate oncogenesis/metastasis driving miRNAs may provide an effective, relatively safer option for cancer therapy. In addition, the high affinity of oligonucleotides to hepatocytes implies that miRNA antagomir therapy might contribute to a favorable approach in treatment of liver diseases. Our results presented here further support the notion that a locked nucleic acid-based inhibition of miR-494 may provide a promising approach for sustaining sufficient

expression of TET protein and multiple invasion-suppressor miRNAs as a novel therapeutic strategy against HCC vascular invasion and recurrence.

*Acknowledgment:* The authors are grateful to Dr. Stephen Welle for critical review.

## References

- Forner A, Llovet JM, Bruix J. Hepatocellular carcinoma. *Lancet* 2012; 379:1245-1255.
- Schlaeger C, Longrich T, Schiller C, Bewerunge P, Mehrabi A, Toedt G, et al. Etiology-dependent molecular mechanisms in human hepatocarcinogenesis. *HEPATOLOGY* 2008;47:511-520.
- El-Serag HB. Hepatocellular carcinoma. *N Engl J Med* 2011;365:1118-1127.
- Bartel DP. MicroRNAs: genomics, biogenesis, mechanism, and function. *Cell* 2004;116:281-297.
- Calin GA, Ferracin M, Cimmino A, Di Leva G, Shimizu M, Wojcik SE, et al. A MicroRNA signature associated with prognosis and progression in chronic lymphocytic leukemia. *N Engl J Med* 2005;353:1793-1801.
- He L, Thomson JM, Hemann MT, Hernando-Monge E, Mu D, Goodson S, et al. A microRNA polycistron as a potential human oncogene. *Nature* 2005;435:828-833.
- Ma L, Teruya-Feldstein J, Weinberg RA. Tumour invasion and metastasis initiated by microRNA-10b in breast cancer. *Nature* 2007;449:682-688.
- Breving K, Esquela-Kerscher A. The complexities of microRNA regulation: mirandering around the rules. *Int J Biochem Cell Biol* 2010;42:1316-1329.
- Lujambio A, Ropero S, Ballestar E, Fraga MF, Cerrato C, Setien F, et al. Genetic unmasking of an epigenetically silenced microRNA in human cancer cells. *Cancer Res* 2007;67:1424-1429.
- Saito Y, Liang G, Egger G, Friedman JM, Chuang JC, Coetzee GA, Jones PA. Specific activation of microRNA-127 with downregulation of the proto-oncogene BCL6 by chromatin-modifying drugs in human cancer cells. *Cancer Cell* 2006;9:435-443.
- Toyota M, Suzuki H, Sasaki Y, Maruyama R, Imai K, Shinomura Y, Tokino T. Epigenetic silencing of microRNA-34b/c and B-cell translocation gene 4 is associated with CpG island methylation in colorectal cancer. *Cancer Res* 2008;68:4123-4132.
- Kulis M, Esteller M. DNA methylation and cancer. *Adv Genet* 2010; 70:27-56.
- Taberlay PC, Jones PA. DNA methylation and cancer. *Prog Drug Res* 2011;67:1-23.
- Ito S, D'Alessio AC, Taranova OV, Hong K, Sowers LC, Zhang Y. Role of Tet proteins in 5mC to 5hmC conversion, ES-cell self-renewal and inner cell mass specification. *Nature* 2010;466:1129-1133.
- Ko M, Huang Y, Jankowska AM, Pape UJ, Tahiliani M, Bandukwala HS, et al. Impaired hydroxylation of 5-methylcytosine in myeloid cancers with mutant TET2. *Nature* 2010;468:839-843.
- Tahiliani M, Koh KP, Shen Y, Pastor WA, Bandukwala H, Brudno Y, et al. Conversion of 5-methylcytosine to 5-hydroxymethylcytosine in mammalian DNA by MLL partner TET1. *Science* 2009;324:930-935.
- Haffner MC, Chaux A, Meeker AK, Esopi DM, Gerber J, Pellakuru LG, et al. Global 5-hydroxymethylcytosine content is significantly reduced in tissue stem/progenitor cell compartments and in human cancers. *Oncotarget* 2011;2:627-637.
- Yang H, Liu Y, Bai F, Zhang JY, Ma SH, Liu J, et al. Tumor development is associated with decrease of TET gene expression and 5-methylcytosine hydroxylation. *Oncogene* 2013;32:663-669.
- Liu C, Liu L, Chen X, Shen J, Shan J, Xu Y, et al. Decrease of 5-hydroxymethylcytosine is associated with progression of hepatocellular carcinoma through downregulation of TET1. *PLoS One* 2013;8:e62828.
- Chen PJ, Chen DS, Lai MY, Chang MH, Huang GT, Yang PM, et al. Clonal origin of recurrent hepatocellular carcinomas. *Gastroenterology* 1989;96:527-529.
- Barry CT, D'Souza M, McCall M, Safadjou S, Ryan C, Kashyap R, et al. Micro RNA expression profiles as adjunctive data to assess the risk of hepatocellular carcinoma recurrence after liver transplantation. *Am J Transplant* 2012;12:428-437.
- Lim L, Balakrishnan A, Huskey N, Jones KD, Jodari M, Ng R, et al. MicroRNA-494 within an oncogenic microRNA megacluster regulates G1/S transition in liver tumorigenesis through suppression of mutated in colorectal cancer. *HEPATOLOGY* 2014;59:202-215.
- Yoshida K. A subset of microRNAs potentially acts as a convergent hub for upstream transcription factors in cancer cells. *Oncol Rep* 2010; 24:1371-1381.
- Park SM, Gaur AB, Lengyel E, Peter ME. The miR-200 family determines the epithelial phenotype of cancer cells by targeting the E-cadherin repressors ZEB1 and ZEB2. *Genes Dev* 2008;22:894-907.
- Iliopoulos D, Lindahl-Allen M, Polytaichou C, Hirsch HA, Tschichl PN, Struhl K. Loss of miR-200 inhibition of Suz12 leads to polycomb-mediated repression required for the formation and maintenance of cancer stem cells. *Mol Cell* 2010;39:761-772.
- Shimono Y, Zabala M, Cho RW, Lobo N, Dalerba P, Qian D, et al. Downregulation of miRNA-200c links breast cancer stem cells with normal stem cells. *Cell* 2009;138:592-603.
- Kim T, Veronese A, Pichiorri F, Lee TJ, Jeon YJ, Volinia S, et al. p53 regulates epithelial-mesenchymal transition through microRNAs targeting ZEB1 and ZEB2. *J Exp Med* 2011;208:875-883.
- Davalos V, Moutinho C, Villanueva A, Boque R, Silva P, Carneiro F, Esteller M. Dynamic epigenetic regulation of the microRNA-200 family mediates epithelial and mesenchymal transitions in human tumorigenesis. *Oncogene* 2012;31:2062-2074.
- Neves R, Scheel C, Weinhold S, Honisch E, Iwaniuk KM, Trompeter HI, et al. Role of DNA methylation in miR-200c/141 cluster silencing in invasive breast cancer cells. *BMC Res Notes* 2010;3:219-219.
- Vrba L, Jensen TJ, Garbe JC, Heimark RL, Cress AE, Dickinson S, et al. Role for DNA methylation in the regulation of miR-200c and miR-141 expression in normal and cancer cells. *PLoS One* 2010;5:e8697.
- Nestor CE, Ottaviano R, Reddington J, Sproul D, Reinhardt D, Dunican D, et al. Tissue type is a major modifier of the 5-hydroxymethylcytosine content of human genes. *Genome Res* 2012;22:467-477.
- Langemeijer SMC, Kuiper RP, Berends M, Knops R, Aslanyan MG, Massop M, et al. Acquired mutations in TET2 are common in myelodysplastic syndromes. *Nat Genet* 2009;41:838-842.
- Wang X, Zhang X, Ren XP, Chen J, Liu H, Yang J, et al. MicroRNA-494 targeting both proapoptotic and antiapoptotic proteins protects against ischemia/reperfusion-induced cardiac injury. *Circulation* 2010; 122:1308-1318.
- Romano G, Acunzo M, Garofalo M, Di Leva G, Cascione L, Zanca C, et al. MiR-494 is regulated by ERK1/2 and modulates TRAIL-induced apoptosis in non-small-cell lung cancer through BIM downregulation. *Proc Natl Acad Sci U S A* 2012;109:16570-16575.
- Liu L, Jiang Y, Zhang H, Greenlee AR, Han Z. Overexpressed miR-494 down-regulates PTEN gene expression in cells transformed by anti-benzo(a)pyrene-trans-7,8-dihydrodiol-9,10-epoxide. *Life Sci* 2010; 86:192-198.
- Ohdaira H, Sekiguchi M, Miyata K, Yoshida K. MicroRNA-494 suppresses cell proliferation and induces senescence in A549 lung cancer cells. *Cell Prolif* 2012;45:32-38.
- Olaru AV, Ghiur G, Yamanaka S, Luvsanjav D, An F, Popescu I, et al. MicroRNA down-regulated in human cholangiocarcinoma control cell cycle through multiple targets involved in the G1/S checkpoint. *HEPATOLOGY* 2011;54:2089-2098.
- Li L, Li Z, Kong X, Xie D, Jia Z, Jiang W, et al. Down-regulation of microRNA-494 via loss of SMAD4 increases FOXM1 and beta-catenin



- signaling in pancreatic ductal adenocarcinoma cells. *Gastroenterology* 2014;147:485-497.e18.
39. Braconi C, Huang N, Patel T. MicroRNA-dependent regulation of DNA methyltransferase-1 and tumor suppressor gene expression by interleukin-6 in human malignant cholangiocytes. *HEPATOLOGY* 2010;51:881-890.
  40. Duursma AM, Kedde M, Schrier M, le Sage C, Agami R. miR-148 targets human DNMT3b protein coding region. *RNA* 2008;14:872-877.
  41. Huang J, Wang Y, Guo Y, Sun S. Down-regulated microRNA-152 induces aberrant DNA methylation in hepatitis B virus-related hepatocellular carcinoma by targeting DNA methyltransferase 1. *HEPATOLOGY* 2010;52:60-70.
  42. Pan W, Zhu S, Yuan M, Cui H, Wang L, Luo X, et al. MicroRNA-21 and microRNA-148a contribute to DNA hypomethylation in lupus CD4+ T cells by directly and indirectly targeting DNA methyltransferase 1. *J Immunol* 2010;184:6773-6781.
  43. **Zhao S, Wang Y, Liang Y**, Zhao M, Long H, Ding S, et al. MicroRNA-126 regulates DNA methylation in CD4+ T cells and contributes to systemic lupus erythematosus by targeting DNA methyltransferase 1. *Arthritis Rheum* 2011;63:1376-1386.
  44. **Jin SG, Jiang Y, Qiu R**, Rauch TA, Wang Y, Schackert G, et al. 5-Hydroxymethylcytosine is strongly depleted in human cancers but its levels do not correlate with IDH1 mutations. *Cancer Res* 2011;71:7360-7365.
  45. Kudo Y, Tateishi K, Yamamoto K, Yamamoto S, Asaoka Y, Ijichi H, et al. Loss of 5-hydroxymethylcytosine is accompanied with malignant cellular transformation. *Cancer Sci* 2012;103:670-676.
  46. Shih AH, Abdel-Wahab O, Patel JB, Levine RL. The role of mutations in epigenetic regulators in myeloid malignancies. *Nat Rev Cancer* 2012;12:599-612.
  47. **Figueroa ME, Abdel-Wahab O, Lu C**, Ward PS, Patel J, Shih A, et al. Leukemic IDH1 and IDH2 mutations result in a hypermethylation phenotype, disrupt TET2 function, and impair hematopoietic differentiation. *Cancer Cell* 2010;18:553-567.
  48. **Hsu CH, Peng KL**, Kang ML, Chen YR, Yang YC, Tsai CH, et al. TET1 suppresses cancer invasion by activating the tissue inhibitors of metalloproteinases. *Cell Rep* 2012;2:568-579.
  49. Zimmermann TS, Lee ACH, Akinc A, Bramlage B, Bumcrot D, Fedoruk MN, et al. RNAi-mediated gene silencing in non-human primates. *Nature* 2006;441:111-114.
  50. Braconi C, Patel T. Non-coding RNAs as therapeutic targets in hepatocellular cancer. *Curr Cancer Drug Targets* 2012;12:1073-1080.

Author names in bold designate shared co-first authorship.

## Supporting Information

Additional Supporting Information may be found at <http://onlinelibrary.wiley.com/doi/10.1002/hep.27816/supinfo>.